Antiviral Research 161 (2019) 108–115

Contents lists available at ScienceDirect

Antiviral Research

journal homepage: www.elsevier.com/locate/antiviral

A neonatal mouse model of Enterovirus D68 infection induces both interstitial pneumonia and acute flaccid myelitis

Shiyang Sun[a,b,1], Lianlian Bian[b,1], Fan Gao[b,1], Ruixiao Du[b], Yalin Hu[c], Ying Fu[b], Yao Su[b], Xing Wu[b,**], Qunying Mao[b,***], Zhenglun Liang[b,*]

[a] Institute of Medicinal Biotechnology Chinese Academy of Medical Sciences, Peking Union Medical College (PUMC), Beijing, China
[b] National Institute for Food and Drug Control, Beijing, China
[c] Hualan Biological Engineering Inc, Xinxiang, China

ARTICLE INFO

Keywords:
Enterovirus D68
Neonatal mouse model
Infection
Interstitial pneumonia
Acute flaccid myelitis

ABSTRACT

Enterovirus D68 (EV-D68) is a causative agent of recent outbreaks of severe respiratory illness, pneumonia and acute flaccid myelitis (AFM) worldwide. The study of the pathogenesis, vaccines and anti-viral drugs for EV-D68 infection has been reported. Given the previously described mouse model of EV-D68, we sought to establish a neonatal mice model inducing both pneumonia and AFM. The neonatal BALB/c mice were inoculated intraperitoneally with the EV-D68 strain (named15296-virus) which was produced by the reverse genetics method. The infected mice displayed limb paralysis, tachypnea and even death, which were similar to the clinical symptoms of human infections. Moreover, the results of histopathologic examination and immunohistochemical staining showed acidophilic necrosis in the muscle, the spinal cord and alveolar wall thickening in the lung, indicating that EV-D68 exhibited strong tropism to the muscles, spinal cord and lung. Furthermore, the results of real-time PCR also suggested that the viral loads in the blood, spinal cord, muscles and lung were higher than those in other tissues at different time points post-infection. Additionally, the neonatal mouse model was used for evaluating the EV-D68 infection. The results of the anti-serum passive and maternal antibody protection indicated that the neonatal mice could be protected against the EV-D68 challenge, and displayed that both the serum of 15296-virus and prototype-virus (Fermon) were performing a certain cross-protective activity against the 15296-virus challenge. In summary, the above results proved that our neonatal mouse model possessed not only the interstitial pneumonia and AFM simultaneously but also a potentiality to evaluate the protective effects of EV-D68 vaccines and anti-viral drugs in the future.

1. Introduction

Human Enteroviruses (HEVs) are classified into 12 species, including Enterovirus A through J and rhinovirus A through C, Enterovirus D68 (EV-D68) belongs to Enterovirus D (Huang et al., 2015). As a non-enveloped, positive-sense, single-stranded RNA virus, EV-D68 was first isolated from four hospitalized pediatric patients with lower respiratory tract infection in California, USA, in 1962 (Schieble et al., 1967). Although it was identified around 50 years ago, EV-D68 still did not attract much global attention until several clusters of severe respiratory illnesses occurred in Asia, Europe, and USA during 2008–2010 (Centers for Disease and Prevention, 2011; Hasegawa et al., 2011; Imamura et al., 2011; Kaida et al., 2011; Rahamat-Langendoen et al., 2011). The largest and most widespread EV-D68 outbreak occurred in USA in 2014, which involved more than 1000 cases of severe respiratory disease from almost all states, including 14 deaths by January 2015 (https://www.cdc.gov/non-polio-enterovirus/about/ev-d68.html#outbreak). According to the epidemiological surveys, there were

Abbreviations: EV-D68, Enterovirus D68; AFM, Acute flaccid myelitis; URTIs, Upper respiratory tract infections; LRTIs, Lower respiratory tract infections; RD cells, Human Rhabdomyosarcoma; H&E, Histopathological Examination; IHC, Immunohistochemical analysis; EV-A71, Enterovirus 71; CV-A16, Coxsackievirus A16

* Corresponding author. National Institutes for Food and Drug Control, No. 31, Huatuo Street, Beijing, 102629, China.
** Corresponding author. National Institutes for Food and Drug Control, No. 31, Huatuo Street, Beijing, 102629, China..
*** Corresponding author. National Institutes for Food and Drug Control, No. 31, Huatuo Street, Beijing, 102629, China.
E-mail addresses: sunbaoshiyang@163.com (S. Sun), bianlian2015@126.com (L. Bian), gaofan0914@qq.com (F. Gao), 18600674038@163.com (R. Du), 903818633@qq.com (Y. Hu), 863614216@qq.com (Y. Fu), justsuyao@163.com (Y. Su), eastarwx@163.com (X. Wu), maoqunying@126.com (Q. Mao), lzhenglun@126.com (Z. Liang).
[1] These authors contributed equally to this work.

https://doi.org/10.1016/j.antiviral.2018.11.013
Received 8 June 2018; Received in revised form 1 November 2018; Accepted 26 November 2018
Available online 29 November 2018

more than 2000 EV-D68 associated cases in 20 countries in 2014 (Holm-Hansen et al., 2016), which has driven EV-D68 to become an important pathogen of severe respiratory illnesses.

During the epidemic of EV-D68, the cases of neurological symptoms such as AFM with a striking resemblance to poliomyelitis increased and occurred primarily in young children (Greninger et al., 2015; Messacar et al., 2016; Sejvar et al., 2016). The coincidental outbreak of AFM and EV-D68 associated respiratory illnesses demonstrated a possible causal association between them (Messacar et al., 2016; Sejvar et al., 2016). Besides the severity of AFM, EV-D68 could lead to severe acute upper respiratory tract infections (URTIs), lower respiratory tract infections (LRTIs) and pneumonia, which seriously threatened children's health. EV-D68-related pneumonia had been reported in Japan, France, Italy, USA, Mexico and China (ElBadry et al., 2016; Esposito et al., 2015; Hellferscee et al., 2017; Lang et al., 2014; Vazquez-Perez et al., 2016; Zhang et al., 2015). A case report also indicated that children could display both pneumonia and AFM after EV-D68 infection (Kreuter et al., 2011). As a consequence, the clinical symptoms of pneumonia and AFM associated with EV-D68 infection should be paid more public attention.

So far, the mouse model of pneumonia (Charu Rajput et al., 2017a, 2017b; Patel et al., 2016; Zheng et al., 2017) and AFM (Hixon et al., 2017a, 2017b; Morrey et al., 2018; Zhang et al., 2018) has been established. According to these studies, EV-D68 produced by a plasmid-based reverse genetics system, was intraperitoneally (i.p.) inoculated into neonatal BALB/c mice to establish the infected mouse model showing both interstitial pneumonia and AFM, which was evaluated by viral loads, histopathologic examination (HE) and immunohistochemical (IHC) staining. Furthermore, using this mouse model, the anti-serum passive protection and maternal antibody protection were evaluated.

2. Materials and methods

2.1. Cell, virus, and antibodies

Human rhabdomyosarcoma (RD) was purchased from ATCC (Manassas, Virginia, USA). The complete genome was isolated from a pneumonia case, on August 5, 2014, in China (Beijing-R0132, GenBank accession no. KP240936) (Zhang et al., 2015). According to the alignment of partial VP1 sequences (339 bp), the strain belongs to subclade B2 (Eshaghi et al., 2017) and genome was constructed under the pBluescriptII SK-vector (Tai he gene, Beijing, China). The virus was created through the reverse genetics method described previously (Sun et al., 2018a), which had been stored at the China General Microbiological Culture Collection Center (CGMCC), and named 15296-virus. The prototype strain Fermon was purchased from ATCC (GenBank accession no. AY426531). All viruses were grown in RD cells, subjected to three freeze-thaw cycles, clarified by centrifugation at 3900 × *g* for 10 min at 4 °C, filtered through a syringe filter (0.2 μm; Pall Corporation, Germany) and stored at −80 °C. Titers of viral stocks were determined by tissue culture infective dose ($TCID_{50}$) assay: 15296-virus: 1×10^8 $TCID_{50}$/mL; Fermon strain: 3.16×10^7 $TCID_{50}$/mL. The EV-D68 VP1 antibody (GT1843) was purchased from Bio-way Company.

2.2. Mouse infection experiments

All animal experiments were carried out in accordance with the guidelines of the National Institute for Food and Drug Control for the Care and Use of Laboratory Animals. To compare the susceptibility of EV-D68 infection, neonatal mice from KunMing (KM), NIH, C57BL/6, ICR, and BALB/c mice (n = 8–10) were injected i.p. with 10^7 $TCID_{50}$/mL of 15296-virus (in a 100 μL volume) or mice given 100 μL of Dulbecco's modified eagle medium (DMEM), which were examined daily for survival and clinical signs for 16 days post infection.

To determine the median lethal dose (LD_{50}), neonatal mice were inoculated i.p. with 15296-virus in different doses and DMEM as a control. Mice were monitored daily for survival and clinical signs for 16 days. Clinical scores were graded as follows: 0, healthy; 1, lethargy and reduced mobility; 2, fore limb paralysis; 3, hind limb paralysis; 4, tachypnea and moribund; 5, death (Table 1). The LD_{50} was calculated as described by Reed and Muench (Reed LJ, 1938), and the dose of 10^7 $TCID_{50}$/100 μL ($5LD_{50}$) was selected as the challenge dose in the following study.

Table 1
Grading score for clinical signs of 15296-virus infected mice.

Grade	Clinical sign(s)
0	Healthy
1	Lethargy and reduced mobility
2	Fore limb paralysis
3	Hind limb paralysis
4	Tachypnea and moribund
5	Death

Table 2
Comparison of the sensitivity of the different mouse strains to 15296-virus. '−' no sign of clinical disease; '+' weak sign of clinical disease; '+ + +' severe sign of clinical disease and death.

Mouse strains (Number)	Clinical sign	Survival (Number)
KM(9)	–	9
NIH(9)	–	9
C57BL/6 (8)	+	8
ICR(9)	+ + +	0
BALB/c (10)	+ + +	0

2.3. Histopathological examination and immunohistochemical staining

The neonatal BALB/c mice were i.p. injected with culture medium or $5LD_{50}$ of 15296-virus. The moribund mouse was euthanized, and various tissues including brain, liver, kidney, intestine, heart, lung, (fore and hind) limb muscles, paraspinal muscle, and spinal cord were collected, and then fixed in 4% paraformaldehyde for 24 h. The histopathological examination (H&E) and Immunohistochemical (IHC) analysis were followed from the previous study (Mao et al., 2012). The detection antibody targeting theVP1 region of EV-D68 was diluted with 1:2000.

2.4. Detection of the 15296-virus load in tissues of infected mice

Samples were collected from the neonatal BALB/c mice i.p. challenged with the culture medium or $5LD_{50}$ of 15296 virus. At days 1, 3, 5 and 7 post-infection (dpi), the mice were euthanized and blood samples were harvested, and stored at −80 °C. The tissues were aseptically removed, weighed and homogenized with a mechanical homogenizer (Sonics & Materials, Inc. Australia) in sterile phosphate-buffered saline (10%, wt/vol). After centrifugation, the total RNA was extracted from blood and tissue supernatants with Mag Max viral isolation kit (Ambion Inc., Austin, TX) by following the manufacturer's recommended protocols, The virus loads were determined by real-time quantitative reverse transcriptase PCR following the conditions in the previous study (Piralla et al., 2015). The complete genome plasmid described previously was used as a standard, and a standard curve generated from serially diluted samples was used to quantify the copies of 15296-virus. The loads of different samples were expressed as $\log_{10}$ RNA copies/mg for the tissues and $\log_{10}$ RNA copies/mL for blood.

2.5. The passive protective efficacy of immune serum

The immune serum was obtained by the injecting 6 week-old female BALB/c mice i.p. with the experimental 15296-virus (1×10^8 $TCID_{50}$/

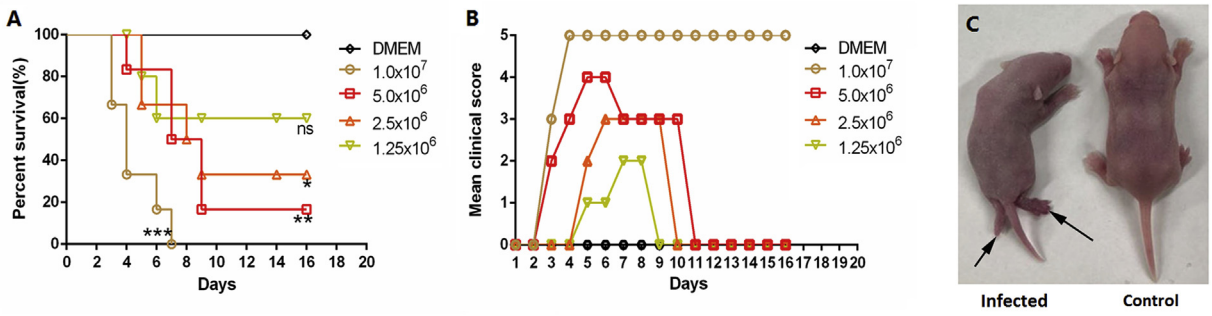

Fig. 1. Dose dependence of 15296-virus induced clinical signs and mortality. Neonatal BALB/c mice (n = 8–10/group) were inoculated i.p. with different doses of 15296-virus (1.25×10^6, 2.5×10^6, 5.0×10^6 and 1.0×10^7 $TCID_{50}$/100 μL). The control mice were injected with DMEM. The survival rate of the mice in 16 days post-infection (dpi) (A) (***, $P < 0.001$; **, $P < 0.01$; *, $P < 0.05$); the clinical scores of the mice in 16 dpi (B); the mouse infected with 15296-virus (on the left) exhibited limb paralysis, while the one injected with DMEM (on the right) was healthy (C). Three independent experiments were performed in duplicate, and the representative data were presented.

mL) and adding 37% formaldehyde (Sinopharm Group, Beijing, China) to the suspensions of the virus for a final formaldehyde concentration of 1/4000. The viral suspension was then incubated at 37 °C for 3 days (Martin et al., 2003). After being immunized for 2 doses at day 0 and 14, the blood was collected on day 21 after the first injection and stored at 4 °C for 24 h, then centrifuged at 5000 rpm for 10 min to separate the serum. The neutralizing antibody (NtAb) titer against EV-D68 was detected by micro-neutralization assay (Sun et al., 2018b). The Fermon immune serum was prepared by the same method. In addition, the human (adult) serum from Human provided by Hualan Biological Engineering Inc, was used as a positive control in the following study (Sun et al., 2018a). The NtAb titers of the 15296-virus were used to detect these three serums, only. The NtAb of 15296-virus immune serum, Fermon immune serum and Human (adult) serum were 1:2048, 1:1024, and 1:256, respectively.

In the passive protective assays, the 15296-virus immune serum sample was diluted from 10- to 10,000-fold and incubated with $5LD_{50}$ of the 15296-virus at 37 °C for 90 min. The neonatal mice were challenged with the sera-virus mixture (i.p.). The 10-fold diluted Fermon immune serum and human (adult) serum were each incubated with $5LD_{50}$ of the 15296-virus respectively, and then the neonatal mice were challenged with the mixture (i.p.) and monitored daily for survival and clinical scores for 16 days.

For further evaluation of the protective efficacy of serum antibodies, neonatal BALB/c mice were inoculated i.p. from 10- to 10,000-fold dilution of the 15296 serum. The neonatal mice were challenged with $5LD_{50}$ of the 15296-virus (i.p.) 90 min after inoculating. The 10-fold diluted Fermon immune serum and human (adult) serum were processed in the same manner. Mice were monitored daily for survival and clinical scores for 16 days.

2.6. The protective efficacy of maternal transferred antibody

To evaluate the efficacy of maternal transferred antibody, 6 week old female BALB/c mice were randomly divided into 5 groups (n = 5 per group), which were immunized with live 15296-virus, live Fermon virus, inactivated 15296-virus, inactivated Fermon virus or DMEM on days 0 and 14, respectively. After immunized with the first dose, the female's mice were housed with males within the same cage for impregnation. Three weeks later, the born neonatal mice were challenged with a lethal dose of $5LD_{50}$ of 15296-virus (i.p.). Mice were monitored daily for survival and clinical scores for 16 days.

2.7. Statistical analysis

All results were obtained with at least three replicates and expressed as the mean standard deviation (SD). All statistical analyses were performed with the Prism version 6.0 software package (GraphPad San Diego, CA,USA).

3. Results

3.1. Comparison of the sensitivity of the different mouse strains to 15296-virus

KM, NIH, C57BL/6, ICR and BALB/c mice (n = 8–10) were adopted to compare the susceptibility of EV-D68 infection, of which the neonatal mice were used in this study. Although the respiratory tract was the natural route of infection, intranasal infection in neonatal mice was difficult to operate. Thus, i.p. injections were used instead. The results showed that the infected KM and NIH mice exhibited no sign of disease and all survived as well as the DMEM group (data not shown). The C57BL/6 mice displayed weak signs, while the ICR and BALB/c mice showed severe signs and even death (Table 2). The BALB/c mice belonged to an inbred mouse strain with the same genotype and phenotype as a result of continuous inbreeding and had the same response to external stimuli, which could increase the reliability and repeatability of the experiment (Li et al., 2017). Therefore, we selected the BALB/c mice in the following study.

3.2. Dose-dependence of 15296-virus infection presented in neonatal mice

To evaluate the dose-dependent relationship, all mice injected with the dose of 1.0×10^7 $TCID_{50}$/100 μL were dead at 7 dpi, while in the 1.25×10^6, 2.5×10^6 and 5.0×10^6 $TCID_{50}$/100 μL groups, the survival rates were 60%, 35%, and 18%, respectively (Fig. 1A and B). The mean clinical score of the 1.0×10^7 $TCID_{50}$/100 μL group was higher than other groups, while the infected mice of the 1.25×10^6, 2.5×10^6 and 5.0×10^6 $TCID_{50}$/100 μL groups recovered in 9–11 dpi. These results suggested that there was a significant positive correlation between the infectious dose of 15296-virus and the mortality of infected mice. As shown in Fig. 1C, limb weakness and paralysis were induced in the mice after a lethal challenge dose of 15296-virus.

3.3. Histopathological examination and immunohistochemical staining of 15296-virus infected mice

To determine the pathological damage of 15296-virus infection in mice, the results of H&E staining of tissues from the moribund mice revealed severe acidophilic necrosis of muscular tissues such as limb muscles and paraspinal muscles compared to the normal tissues of the control mice (Fig. 2A–F). More importantly, the infected mice showed interstitial pneumonia in the lung (Fig. 2G–H) and pathological lesions in the nervous tissues (Fig. 2I–L). The results of IHC confirmed the positive reaction in (Fig. 3A–F) limb muscle, paraspinal muscle (Fig. 3G–H), lung and (Fig. 3I–J) spinal cord with the anti-EV-D68 VP1

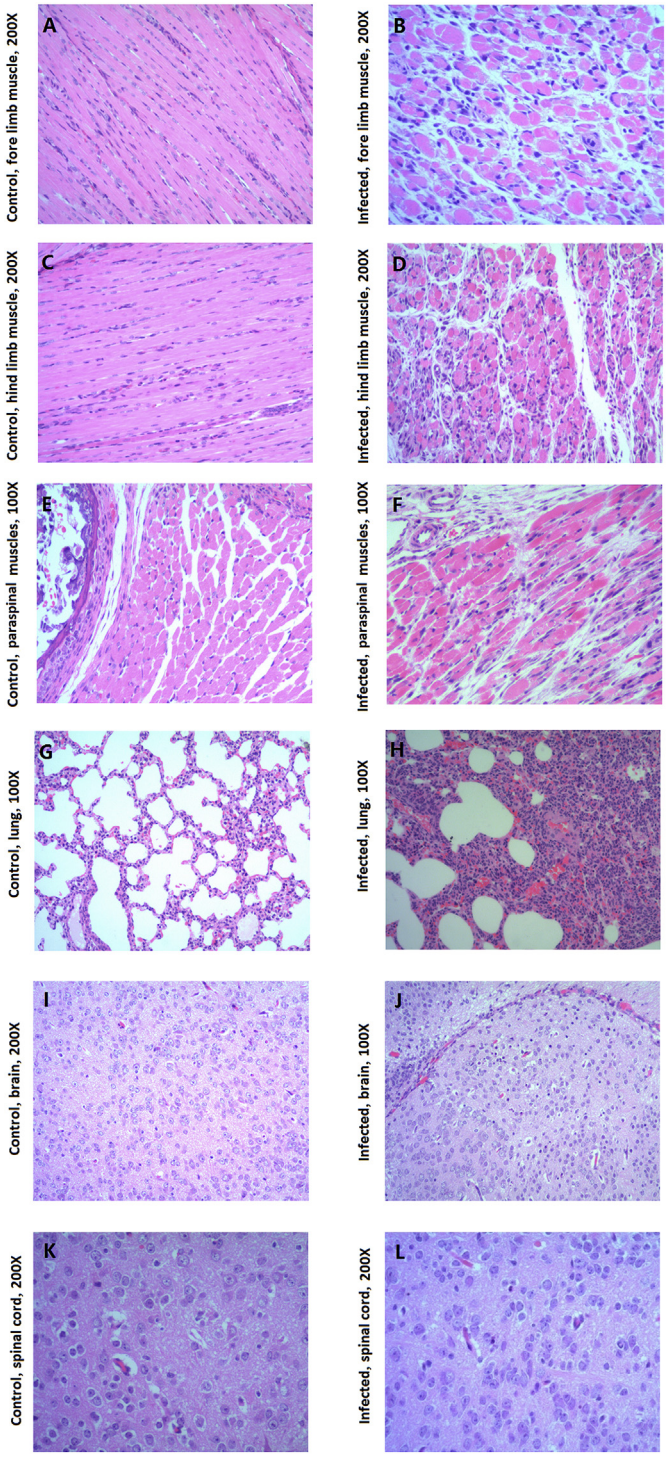

Fig. 2. Histological examination of various tissues from control mice and infected moribund mice. Acidophilic necrosis of limb muscle and paraspinal muscle (A–F); interstitial pneumonia of infected mice (G–H); the pathological changes in nervous system, including acidophilic necrosis of nerve cell in cerebral cortex and spinal cord (I–L).

antibody. However, no pathological changes were observed in other tissues of the infected mice, including liver, kidney, intestine or heart. The results of H&E and IHC demonstrated that the infection of 15296-virus caused the pathological damage in the mice.

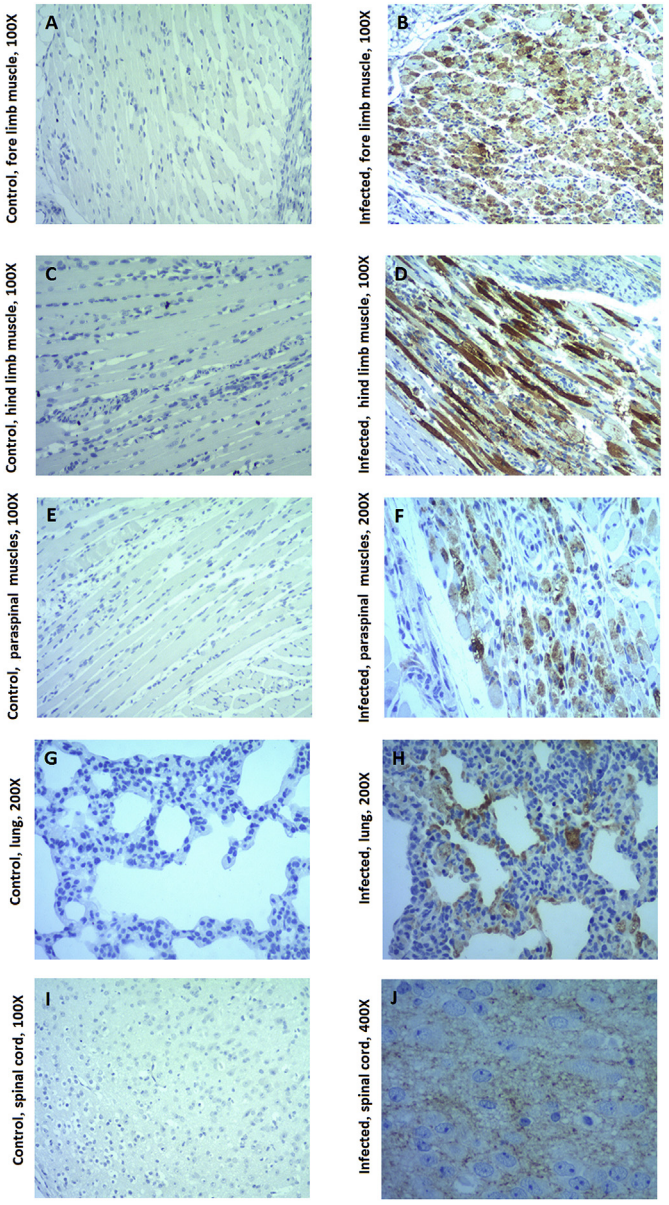

Fig. 3. Immunohistochemical staining of various tissues from control mice and infected moribund mice. The results of IHC staining with anti-EV-D68 VP1 antibody showed positive reaction in limb muscle and paraspinal muscle (A–F), lung (G–H), and spinal cord (I–J).

3.4. Viral loads in tissues of 15296-virus infected mice

To further understand the spread route of 15296-virus in the infected mice, the viral loads in blood and different tissues were detected by real-time PCR. As shown in Fig. 4, the viral loads were hardly detected in the brain, heart or intestine at 1 dpi, while the virus RNA in blood, lung, spinal cord and muscle was at a level 1.26×10^4–1.0×10^6/mL or copies/mg. From 3 to 7 dpi, the viral loads in blood and other tissues could be continuously detected. The results demonstrated that all the tissues could be infected with 15296-virus at the medium term of infection. However, the higher amount of the15296-virus RNA was detected in blood, muscle, lung and spinal cord throughout the experiment, suggesting that EV-D68 exhibited a strong tropism to the nervous tissues, muscles and respiratory system, which was consistent with the H&E and IHC results (Figs. 2 and 3).

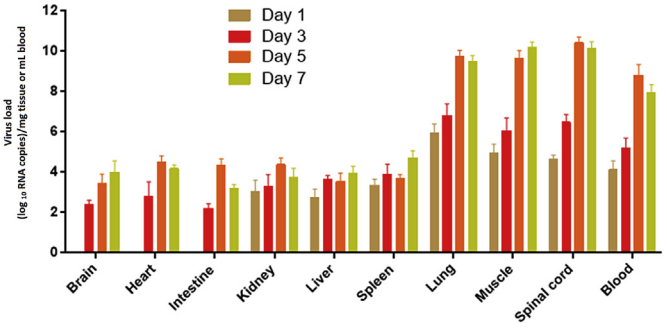

Fig. 4. Tissue viral loads in 15296-virus infected mice. Samples of blood, brain, heart, intestine, kidney, liver, lung, muscle, spinal cord, and spleen were collected from infected mice i.p. challenged with 5 LD_{50} of 15296-virus at 1, 3, 5 and 7 dpi (n = 3 per time point) or control mice given DMEM at 0 days post-infection. Viral load was measured by real-time PCR, and the results represent the mean viral load ± SD.

3.5. Anti-serum passive protection against 15296-virus challenge

To test the passive protective efficacy of anti-15296-virus serum, we chose two different assays. Firstly, as shown in Fig. 5, the protective efficacy of neutralizing serum with 1:10 diluted was 100%, which presented a dose-effect relationship between the neutralizing antibody and the survival rate. The infected mice in the 1:10 diluted group showed no clinical signs, while the mice in the 1:100 and 1:1000 diluted groups recovered in 6–10 dpi. All mice in the 10,000-fold diluted group died within 8 days. Both the Fermon immune serum and Human (adult) serum displayed high-efficiency neutralizing capacity *in vitro*, and the protective efficacy for both was 100%.

In the second test, the protective efficacy of the neutralizing serum with 10-fold dilution was 100% survival. With the neutralizing serum dilution increased, the neonatal BALB/c mice survival rates were about 60% (100-fold diluted group) and 15% (1000-fold diluted group) (Fig. 6). All mice in the 10,000-fold diluted group died within 8 days, similarly to the DMEM group. No clinical signs were found in the 10-fold diluted group, while the infected mice in the 100-fold and 1000-fold diluted groups recovered in 10–11 dpi. The Fermon immune serum and Human (adult) serum with 10-fold diluted ratio also revealed excellent protective efficacy. The passive protective efficacy emerged as a certain cross-protective activity of these three serums against the lethal challenge of the15296-virus.

3.6. Maternal antibody protection against 15296-virus challenge

To determine whether maternal antibodies had a protective effects against the 15296-virus challenge, the neonatal mice were infected with 5LD_{50} of 15296-virus (i.p.). The results in Fig. 7 revealed that four groups provided 100% survival rate after being challenged with the 15296-virus. In contrast, the control group died within 6 dpi. These results demonstrated that maternal antibodies could markedly increase the survival rate of mice with the 15296-virus challenge.

4. Discussion

A suitable animal model is a powerful tool to study the pathogenesis and develop the vaccines and anti-viral drugs against infections. As a member of the group A Human Enterovirus (HEV-A), different animal models of Enterovirus 71 (EV-A71) infection had been successfully established, which strongly promoted the development of EV-A71 vaccines (Caine et al., 2013; Liu et al., 2011; Sun et al., 2015; Xu et al., 2014). Additionally, with the development of the neonatal mouse model of Coxsackievirus (CV)-A16, CV-A6 and CV-A10 infection, the efficacy of many vaccine candidates and anti-viral reagents has been evaluated (Li et al., 2017; Liu et al., 2014; Mao et al., 2012; Sun et al., 2014; Yang et al., 2015, 2016). In recent years, as one of the HEV-D group, the mouse models of EV-D68 had been established in several studies, which only showed the signs of respiratory tract or AFM (Imamura and Oshitani, 2015). Thus, a more susceptible mouse model

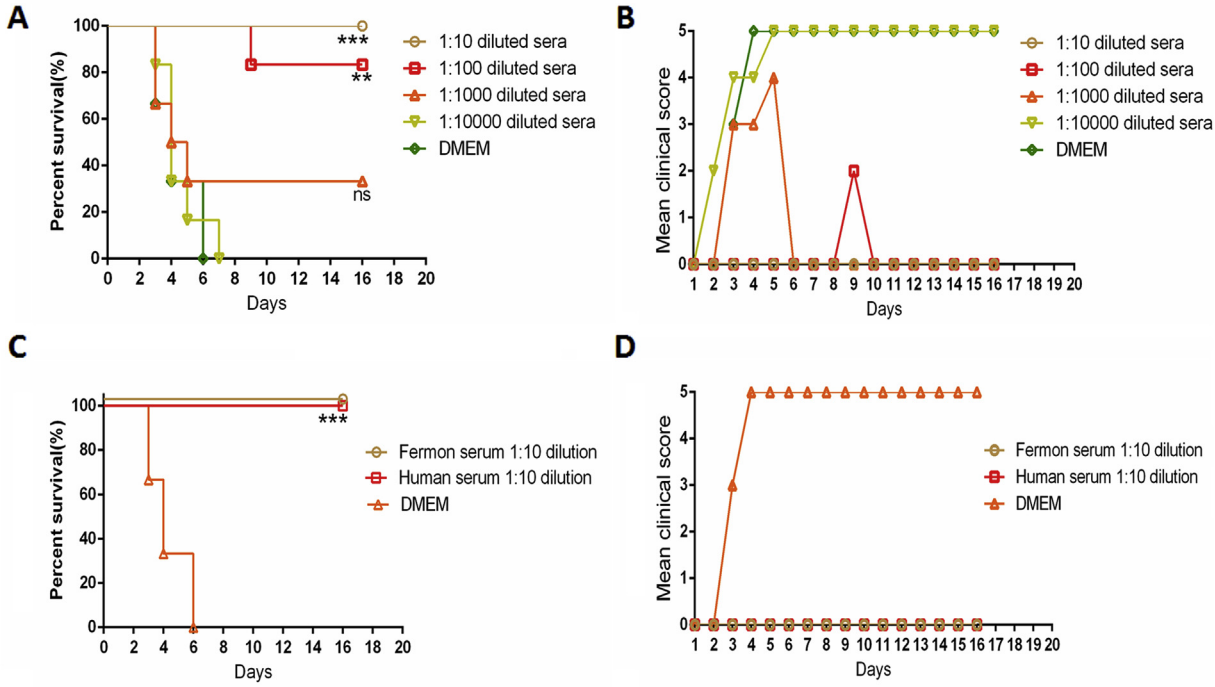

Fig. 5. The passive protective efficacy of neutralizing serum *in vitro*. Neonatal BALB/c mice (n = 6–8 per group) were injected i.p. with 5LD_{50} of 15296-virus which had been neutralized by gradient diluted neutralizing serum from 10- to 10,000-fold *in vitro*. Survival rate (A) and clinical scores (B) were monitored daily for 16 days. The protective efficacy of 1:10 diluted Fermon immune serum and Human (adult) serum was compared (C, D). (***, $P < 0.001$; **, $P < 0.01$; *, $P < 0.05$). Three independent experiments were performed in duplicate, and the representative data were presented.

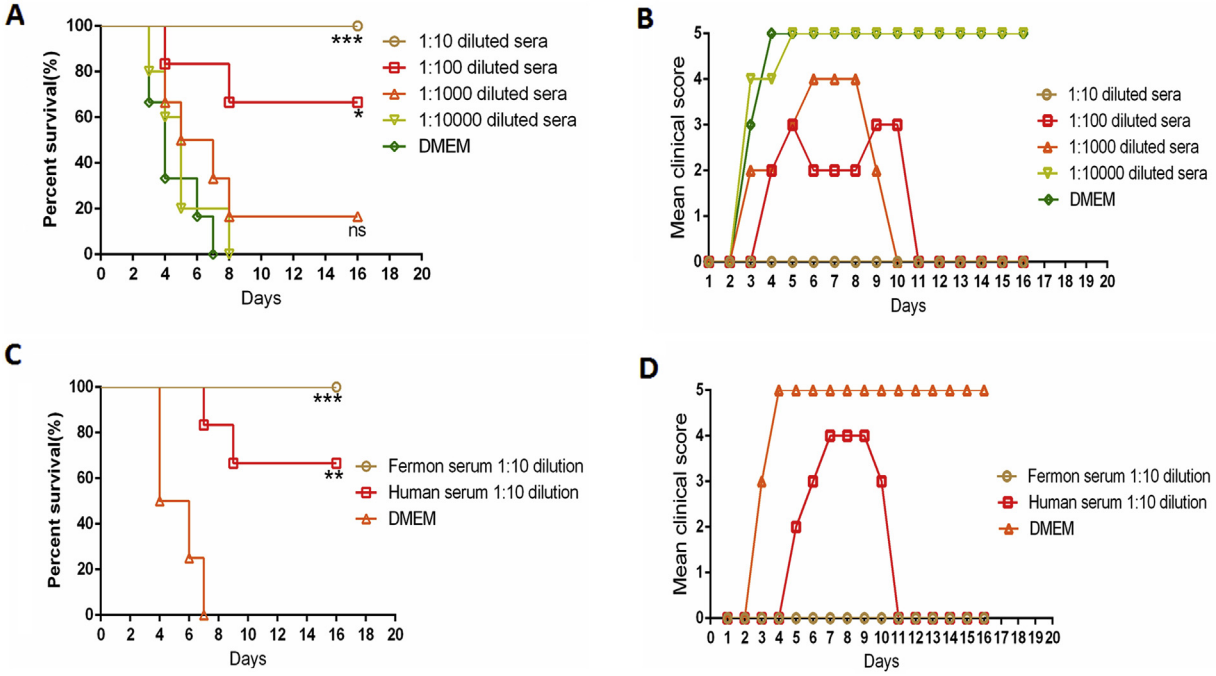

Fig. 6. The passive protective efficacy of neutralizing serum in *vivo*. Neonatal BALB/c mice (n = 6–8 per group) were injected i.p. with gradient diluted neutralizing serum from 10- to 10,000-fold, and then injected with 5 LD_{50} of 15296-virus. Survival rate (A) and clinical scores (B) were monitored daily for 16 days. The protective efficacy of 1:10 diluted Fermon immune serum and Human (adult) serum was compared (C, D). (***, $P < 0.001$; **, $P < 0.01$; *, $P < 0.05$). Three independent experiments were performed in duplicate, and the representative data were presented.

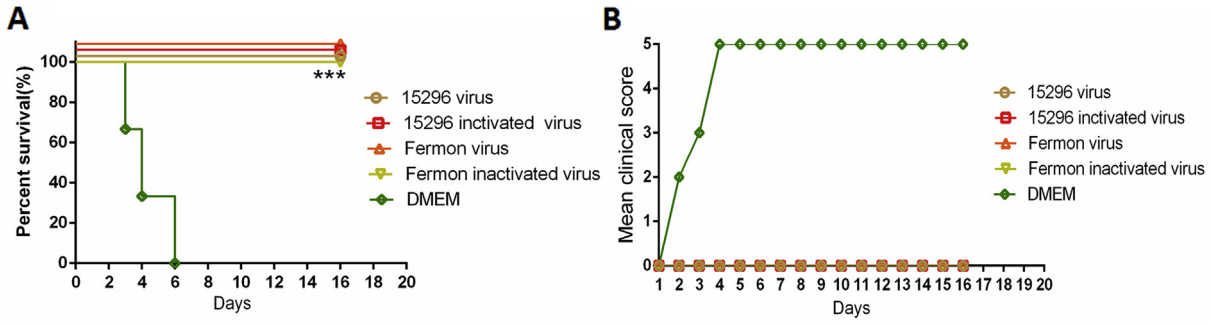

Fig. 7. The protective efficacy of maternal transferred antibody. Six-weeks-old female BALB/c mice were injected i.p. immunized with both the live and formaldehyde-inactivated EV-D68 strain 15296-virus and Fermon. The offspring (n = 6–8/group)were challenged with 5 LD_{50} of 15296-virus. Survival rate (A) and clinical scores (B). (***, $P < 0.001$). Three independent experiments were performed in duplicate, and the representative data were presented.

systematically was needed for the evaluation of vaccines or anti-viral drugs against EV-D68 infection.

EV-D68 infections primarily cause mild to severe respiratory illness (Imamura and Oshitani, 2015). In a recent study, it was reported that EV-D68 virus leads to minimal clinical symptoms in ferrets and this model could induce inflammatory cytokine/chemokine in the lung (Zheng et al., 2017). Patel et al. used the EV-D68 clinical isolates which could cause bronchiolitis, interstitial pneumonia, alveolitis and pulmonary cytokine gene expression in four to six week old female cotton rats (Patel et al., 2016), and Morrey et al. shown that the lung were damaged after infection with EV-D68 virus in different old-age A129 mice (Morrey et al., 2018). In the current study, we found that neonatal BALB/c mice were susceptible to the 15296-virus i.p. infection without virus adaptation. Though the expression of lung-related genes did not detected after challenged 15296-virus, the results of the viral load, H&E and IHC analysis demonstrated that 15296-virus could induce interstitial pneumonia in the neonatal BALB/c mice and was a major site of viral replication. In addition to severe respiratory illness, EV-D68 infections have also been associated with AFM (Hixon et al., 2017b), which affects the nervous system, particularly the spinal cord (Maloney et al., 2015). In this study, the infected mice displayed spinal cord pathological change and viral loads were increased significantly with time, while the viral loads in the brains of infected mice were considerably lower than those in the spinal cord, which indicated that the spinal cord is one of the primary sites for viral replication. However, there was no spinal cord damaged after EV-D68 infection via the respiratory route with the 5-day-osld A129 mice (Morrey et al., 2018), it is not consistent with the previous studies (Hixon et al., 2017b; Zhang et al., 2018)and our result. These may be caused by the age difference or strains. Moreover, the viral load and pathological change were observed in the muscles after being challenged by the 15296-virus, demonstrating that muscle is another major location for viral replication. These results proved that the neonatal mice model was established which induced the paralytic myelitis and pneumonia. Additionally, three mutations which were located in the VP3 (F69L), VP1 (K44N) and 2A (R39G) regions were found and speculated to have a correlation with virulence (detailed data not shown). Future study would be needed to determine and explore the molecular mechanism, and

compare it with the neonatal mice model, which were defective in immune system and limited in operation delivery of anti-viral drug, an adult animal model might be established, which would be more suitable to study the immunopathology and evaluate the efficacy of vaccines and anti-viral drugs.

Vaccination is regarded as one of the most effective defenses against virus infection. Recently, some researchers have tried to develop EV-D68 vaccines and anti-viral drugs (Dai et al., 2018; Hixon et al., 2017a; Zhang et al., 2018), Patel et al. used cotton rats to evaluate the efficacy of vaccine by intramuscular immunization with live VANBT/1 or MO/14/49, showing that the virus could induce strong homologous antibody responses, but a moderate heterologous NtAb response (Patel et al., 2016). Although, the NtAb titers were used with the15296-virus to detect serums only, the formalin-inactivated 15296-virus immune serum, the formalin-inactivated Fermon immune serum and the human (adult) serum could provide a high survival rate compared with the control group, indicating there existed cross-protection between different genotype EV-D68 strains. In addition, the previous cross-sectional seroepidemiological study demonstrated that maternal antibodies of EV-D68 could be transferred across the placenta and provide immunity for newborn infants against EV-D68 infection (Sun et al., 2018a). So far, maternal immunizations have been proven effective for HEV vaccines, such as EV-A71, CV-A16, CV-A6, CV-A10 and EV-D68 (Chung et al., 2008; Li et al., 2017; Mao et al., 2012; Yang et al., 2016; Zhang et al., 2018). In this study, the vaccine candidates were evaluated by the protective efficacy of maternal antibodies against a lethal challenge to the neonatal mice, and the survival rate of the passive protection group and control group were 100% and 0%, respectively. The results also proved that there was cross-protection between different genotype strains. When more circulated strains are isolated, the strains with a better cross activity and stronger immunogenicity should be selected as the candidate strains of EV-D68 vaccine in the future.

In summary, we successfully established the neonatal mouse model for EV-D68 infection, which displayed clinical signs of the interstitial pneumonia and AFM simultaneously. More important, our mouse model shows great potentiality for preliminarily evaluating the protective efficacy of EV-D68 vaccine and anti-viral drugs in the future.

Acknowledgments

The current study was sponsored by the Major Special Projects Funding Program (No. 2016ZX09101120) from the Ministry of Science and Technology of the People's Republic of China. The funders had no role in study design, data collection and analysis, data interpretation, decision to publish, or preparation of the manuscript.

References

Caine, E.A., Partidos, C.D., Santangelo, J.D., Osorio, J.E., 2013. Adaptation of enterovirus 71 to adult interferon deficient mice. PLoS One 8, e59501.
Centers for Disease, C., Prevention, 2011. Clusters of acute respiratory illness associated with human enterovirus 68–Asia, Europe, and United States, 2008-2010. MMWR Morb. Mortal. Wkly. Rep. 60, 1301–1304.
Charu Rajput, J.K.B., Lei, Jing, Han, Mingyuan, Hinde, Joanna, Marc, B., Hershenson, 2017a. Mouse model of human enterovirus D68 asthma exacerbation. Am. J. Respir. Crit. Care Med. 195.
Charu Rajput, J.K.B., Lei, Jing, Han, Mingyuan, Hinde, Joanna, Hershenson, Marc B., McClatchy, John, Evans, Joseph, Hurst, Brett, Tarbet, Bart, 2017b. Development of Murine Model for Enterovirus D68 in AG-129 Mice. Biology Posters. Paper 189.
Chung, Y.C., Ho, M.S., Wu, J.C., Chen, W.J., Huang, J.H., Chou, S.T., Hu, Y.C., 2008. Immunization with virus-like particles of enterovirus 71 elicits potent immune responses and protects mice against lethal challenge. Vaccine 26, 1855–1862.
Dai, W., Zhang, C., Zhang, X., Xiong, P., Liu, Q., Gong, S., Geng, L., Zhou, D., Huang, Z., 2018. A virus-like particle vaccine confers protection against enterovirus D68 lethal challenge in mice. Vaccine 36, 653–659.
ElBadry, M., Lednicky, J., Cella, E., Telisma, T., Chavannes, S., Loeb, J., Ciccozzi, M., Okech, B., Beau De Rochars, V.M., Salemi, M., Morris Jr., J.G., 2016. Isolation of an enterovirus D68 from blood from a child with pneumonia in rural Haiti: close phylogenetic linkage with New York strain. Pediatr. Infect. Dis. J. 35, 1048–1050.
Eshaghi, A., Duvvuri, V.R., Isabel, S., Banh, P., Li, A., Peci, A., Patel, S.N., Gubbay, J.B., 2017. Global distribution and evolutionary history of enterovirus D68, with emphasis on the 2014 outbreak in Ontario, Canada. Front. Microbiol. 8, 257.
Esposito, S., Zampiero, A., Ruggiero, L., Madini, B., Niesters, H., Principi, N., 2015. Enterovirus D68-associated community-acquired pneumonia in children living in Milan, Italy. J. Clin. Virol. 68, 94–96.
Greninger, A.L., Naccache, S.N., Messacar, K., Clayton, A., Yu, G., Somasekar, S., Federman, S., Stryke, D., Anderson, C., Yagi, S., Messenger, S., Wadford, D., Xia, D., Watt, J.P., Van Haren, K., Dominguez, S.R., Glaser, C., Aldrovandi, G., Chiu, C.Y., 2015. A novel outbreak enterovirus D68 strain associated with acute flaccid myelitis cases in the USA (2012-14): a retrospective cohort study. Lancet Infect. Dis. 15, 671–682.
Hasegawa, S., Hirano, R., Okamoto-Nakagawa, R., Ichiyama, T., Shirabe, K., 2011. Enterovirus 68 infection in children with asthma attacks: virus-induced asthma in Japanese children. Allergy 66, 1618–1620.
Hellferscee, O., Treurnicht, F.K., Tempia, S., Variava, E., Dawood, H., Kahn, K., Cohen, A.L., Pretorius, M., Cohen, C., Madhi, S.A., Venter, M., 2017. Enterovirus D68 and other enterovirus serotypes identified in South African patients with severe acute respiratory illness, 2009-2011. Influenza Other Respir. Viruses 11, 211–219.
Hixon, A.M., Clarke, P., Tyler, K.L., 2017a. Evaluating treatment efficacy in a mouse model of enterovirus D68-associated paralytic myelitis. J. Infect. Dis. 216, 1245–1253.
Hixon, A.M., Yu, G., Leser, J.S., Yagi, S., Clarke, P., Chiu, C.Y., Tyler, K.L., 2017b. A mouse model of paralytic myelitis caused by enterovirus D68. PLoS Pathog. 13, e1006199.
Holm-Hansen, C.C., Midgley, S.E., Fischer, T.K., 2016. Global emergence of enterovirus D68: a systematic review. Lancet Infect. Dis. 16, e64–e75. https://www.cdc.gov/non-polio-enterovirus/about/ev-d68.html#outbreak.
Huang, W., Wang, G., Zhuge, J., Nolan, S.M., Dimitrova, N., Fallon, J.T., 2015. Whole-genome sequence analysis reveals the enterovirus D68 isolates during the United States 2014 outbreak mainly belong to a novel clade. Sci. Rep. 5, 15223.
Imamura, T., Fuji, N., Suzuki, A., Tamaki, R., Saito, M., Aniceto, R., Galang, H., Sombrero, L., Lupisan, S., Oshitani, H., 2011. Enterovirus 68 among children with severe acute respiratory infection, the Philippines. Emerg. Infect. Dis. 17, 1430–1435.
Imamura, T., Oshitani, H., 2015. Global reemergence of enterovirus D68 as an important pathogen for acute respiratory infections. Rev. Med. Virol. 25, 102–114.
Kaida, A., Kubo, H., Sekiguchi, J., Kohdera, U., Togawa, M., Shiomi, M., Nishigaki, T., Iritani, N., 2011. Enterovirus 68 in children with acute respiratory tract infections, Osaka, Japan. Emerg. Infect. Dis. 17, 1494–1497.
Kreuter, J.D., Barnes, A., McCarthy, J.E., Schwartzman, J.D., Oberste, M.S., Rhodes, C.H., Modlin, J.F., Wright, P.F., 2011. A fatal central nervous system enterovirus 68 infection. Arch. Pathol. Lab Med. 135, 793–796.
Lang, M., Mirand, A., Savy, N., Henquell, C., Maridet, S., Perignon, R., Labbe, A., Peigue-Lafeuille, H., 2014. Acute flaccid paralysis following enterovirus D68 associated pneumonia, France, 2014. Euro Surveill. 19.
Li, S., Zhao, H., Yang, L., Hou, W., Xu, L., Wu, Y., Wang, W., Chen, C., Wan, J., Ye, X., Liang, Z., Mao, Q., Cheng, T., Xia, N., 2017. A neonatal mouse model of coxsackievirus A10 infection for anti-viral evaluation. Antivir. Res. 144, 247–255.
Liu, L., Zhao, H., Zhang, Y., Wang, J., Che, Y., Dong, C., Zhang, X., Na, R., Shi, H., Jiang, L., Wang, L., Xie, Z., Cui, P., Xiong, X., Liao, Y., Zhao, S., Gao, J., Tang, D., Li, Q., 2011. Neonatal rhesus monkey is a potential animal model for studying pathogenesis of EV71 infection. Virology 412, 91–100.
Liu, Q., Shi, J., Huang, X., Liu, F., Cai, Y., Lan, K., Huang, Z., 2014. A murine model of coxsackievirus A16 infection for anti-viral evaluation. Antivir. Res. 105, 26–31.
Maloney, J.A., Mirsky, D.M., Messacar, K., Dominguez, S.R., Schreiner, T., Stence, N.V., 2015. MRI findings in children with acute flaccid paralysis and cranial nerve dysfunction occurring during the 2014 enterovirus D68 outbreak. AJNR Am. J. Neuroradiol. 36, 245–250.
Mao, Q., Wang, Y., Gao, R., Shao, J., Yao, X., Lang, S., Wang, C., Mao, P., Liang, Z., Wang, J., 2012. A neonatal mouse model of coxsackievirus A16 for vaccine evaluation. J. Virol. 86, 11967–11976.
Martin, J., Crossland, G., Wood, D.J., Minor, P.D., 2003. Characterization of formaldehyde-inactivated poliovirus preparations made from live-attenuated strains. J. Gen. Virol. 84, 1781–1788.
Messacar, K., Schreiner, T.L., Van Haren, K., Yang, M., Glaser, C.A., Tyler, K.L., Dominguez, S.R., 2016. Acute flaccid myelitis: a clinical review of US cases 2012-2015. Ann. Neurol. 80, 326–338.
Morrey, J.D., Wang, H., Hurst, B.L., Zukor, K., Siddharthan, V., Van Wettere, A.J., Sinex, D.G., Tarbet, E.B., 2018. Causation of acute flaccid paralysis by myelitis and myositis in enterovirus-D68 infected mice deficient in interferon alphabeta/gamma receptor deficient mice. Viruses 10.
Patel, M.C., Wang, W., Pletneva, L.M., Rajagopala, S.V., Tan, Y., Hartert, T.V., Boukhvalova, M.S., Vogel, S.N., Das, S.R., Blanco, J.C., 2016. Enterovirus D-68 infection, prophylaxis, and vaccination in a novel permissive animal model, the Cotton Rat (*Sigmodon hispidus*). PLoS One 11, e0166336.
Piralla, A., Girello, A., Premoli, M., Baldanti, F., 2015. A new real-time reverse transcription-PCR assay for detection of human enterovirus 68 in respiratory samples. J. Clin. Microbiol. 53, 1725–1726.
Rahamat-Langendoen, J., Riezebos-Brilman, A., Borger, R., van der Heide, R., Brandenburg, A., Scholvinck, E., Niesters, H.G., 2011. Upsurge of human enterovirus 68 infections in patients with severe respiratory tract infections. J. Clin. Virol 52, 103–106.
Reed LJ, M.H., 1938. A simple method of estimating fifty percent endpoints. Am. J. Epidemiol. 27.
Schieble, J.H., Fox, V.L., Lennette, E.H., 1967. A probable new human picornavirus associated with respiratory diseases. Am. J. Epidemiol. 85, 297–310.
Sejvar, J.J., Lopez, A.S., Cortese, M.M., Leshem, E., Pastula, D.M., Miller, L., Glaser, C., Kambhampati, A., Shioda, K., Aliabadi, N., Fischer, M., Gregoricus, N., Lanciotti, R.,

Nix, W.A., Sakthivel, S.K., Schmid, D.S., Seward, J.F., Tong, S., Oberste, M.S., Pallansch, M., Feikin, D., 2016. Acute flaccid myelitis in the United States, August-December 2014: results of nationwide surveillance. Clin. Infect. Dis. 63, 737–745.

Sun, S., Gao, F., Hu, Y., Bian, L., Wu, X., Su, Y., Du, R., Fu, Y., Zhu, F., Mao, Q., Liang, Z., 2018a. A cross-sectional seroepidemiology study of EV-D68 in China. Emerg. Microb. Infect. 7, 99.

Sun, S., Gao, F., Mao, Q., Shao, J., Jiang, L., Liu, D., Wang, Y., Yao, X., Wu, X., Sun, B., Zhao, D., Ma, Y., Lu, J., Kong, W., Jiang, C., Liang, Z., 2015. Immunogenicity and protective efficacy of an EV71 virus-like particle vaccine against lethal challenge in newborn mice. Hum. Vaccines Immunother. 11, 2406–2413.

Sun, S., Jiang, L., Liang, Z., Mao, Q., Su, W., Zhang, H., Li, X., Jin, J., Xu, L., Zhao, D., Fan, P., An, D., Yang, P., Lu, J., Lv, X., Sun, B., Xu, F., Kong, W., Jiang, C., 2014. Evaluation of monovalent and bivalent vaccines against lethal Enterovirus 71 and Coxsackievirus A16 infection in newborn mice. Hum. Vaccines Immunother. 10, 2885–2895.

Sun, S.Y., Gao, F., Hu, Y.L., Bian, L.L., Mao, Q.Y., Wu, X., Li, J.X., Zhu, F.C., Wang, J.W., Liang, Z.L., 2018b. Seroepidemiology of enterovirus D68 infection in infants and children in Jiangsu, China. J. Infect. 76, 563–569.

Vazquez-Perez, J.A., Ramirez-Gonzalez, J.E., Moreno-Valencia, Y., Hernandez-Hernandez, V.A., Romero-Espinoza, J.A., Castillejos-Lopez, M., Hernandez, A., Perez-Padilla, R., Oropeza-Lopez, L.E., Escobar-Escamilla, N., Gonzalez-Villa, M., Alejandre-Garcia, A., Regalado-Pineda, J., Santillan-Doherty, P., Lopez-Martinez, I., Diaz-Quinonez, A., Salas-Hernandez, J., 2016. EV-D68 infection in children with asthma exacerbation and pneumonia in Mexico City during 2014 autumn. Influenza Other Respir. Viruses 10, 154–160.

Xu, L., He, D., Li, Z., Zheng, J., Yang, L., Yu, M., Yu, H., Chen, Y., Que, Y., Shih, J.W., Liu, G., Zhang, J., Zhao, Q., Cheng, T., Xia, N., 2014. Protection against lethal enterovirus 71 challenge in mice by a recombinant vaccine candidate containing a broadly cross-neutralizing epitope within the VP2 EF loop. Theranostics 4, 498–513.

Yang, L., Li, S., Liu, Y., Hou, W., Lin, Q., Zhao, H., Xu, L., He, D., Ye, X., Zhu, H., Cheng, T., Xia, N., 2015. Construction and characterization of an infectious clone of coxsackievirus A6 that showed high virulence in neonatal mice. Virus Res. 210, 165–168.

Yang, L., Mao, Q., Li, S., Gao, F., Zhao, H., Liu, Y., Wan, J., Ye, X., Xia, N., Cheng, T., Liang, Z., 2016. A neonatal mouse model for the evaluation of antibodies and vaccines against coxsackievirus A6. Antivir. Res. 134, 50–57.

Zhang, C., Zhang, X., Dai, W., Liu, Q., Xiong, P., Wang, S., Geng, L., Gong, S., Huang, Z., 2018. A mouse model of enterovirus D68 infection for assessment of the efficacy of inactivated vaccine. Viruses 10.

Zhang, T., Ren, L., Luo, M., Li, A., Gong, C., Chen, M., Yu, X., Wu, J., Deng, Y., Huang, F., 2015. Enterovirus D68-associated severe pneumonia, China, 2014. Emerg. Infect. Dis. 21, 916–918.

Zheng, H.W., Sun, M., Guo, L., Wang, J.J., Song, J., Li, J.Q., Li, H.Z., Ning, R.T., Yang, Z.N., Fan, H.T., He, Z.L., Liu, L.D., 2017. Nasal infection of enterovirus D68 leading to lower respiratory tract pathogenesis in ferrets (*Mustela putorius furo*). Viruses 9.